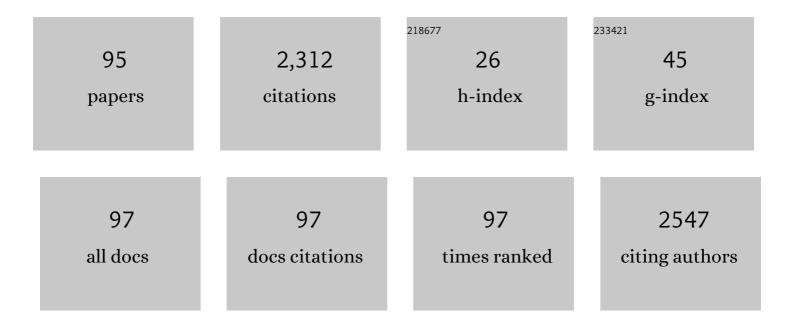
List of Publications by Year in descending order

Source: https://exaly.com/author-pdf/5623013/publications.pdf Version: 2024-02-01



#	Article	IF	CITATIONS
1	The Postspinel Phase Boundary in Mg2SiO4 Determined by in Situ X-ray Diffraction. Science, 1998, 279, 1698-1700.	12.6	251
2	Stability of magnesite and its high-pressure form in the lowermost mantle. Nature, 2004, 427, 60-63.	27.8	234
3	lron partitioning in a pyrolite mantle and the nature of the 410-km seismic discontinuity. Nature, 1998, 392, 702-705.	27.8	137
4	Construction of laser-heated diamond anvil cell system for in situ x-ray diffraction study at SPring-8. Review of Scientific Instruments, 2001, 72, 1289.	1.3	92
5	Phase transformations in serpentine and transportation of water into the lower mantle. Geophysical Research Letters, 1998, 25, 203-206.	4.0	90
6	Post-stishovite phase boundary in SiO2 determined by in situ X-ray observations. Earth and Planetary Science Letters, 2002, 197, 187-192.	4.4	84
7	Preparation of layered organic–inorganic nanohybrid thin films of molybdenum trioxide with polyaniline derivatives for aldehyde gases sensors of several tens ppb level. Sensors and Actuators B: Chemical, 2008, 128, 512-520.	7.8	60
8	Effects of Surface and Bulk Silver on PrMnO _{3+δ} Perovskite for CO and Soot Oxidation: Experimental Evidence for the Chemical State of Silver. ACS Catalysis, 2015, 5, 301-309.	11.2	55
9	Gas response, response time and selectivity of a resistive CO sensor based on two connected CeO2 thick films with various particle sizes. Sensors and Actuators B: Chemical, 2009, 136, 364-370.	7.8	52
10	High pressure and high temperature phase transitions of FeO. Physics of the Earth and Planetary Interiors, 2004, 146, 273-282.	1.9	51
11	Mg/Si ratios of aqueous fluids coexisting with forsterite and enstatite based on the phase relations in the Mg ₂ SiO ₄ -SiO ₂ -H ₂ O system. American Mineralogist, 2004, 89, 1433-1437.	1.9	49
12	Ppm level methane detection using micro-thermoelectric gas sensors with Pd/Al2O3 combustion catalyst films. Sensors and Actuators B: Chemical, 2015, 206, 488-494.	7.8	49
13	Robust hydrogen detection system with a thermoelectric hydrogen sensor for hydrogen station application. International Journal of Hydrogen Energy, 2009, 34, 2834-2841.	7.1	48
14	Ground-State Copper(III) Stabilized by N-Confused/N-Linked Corroles: Synthesis, Characterization, and Redox Reactivity. Journal of the American Chemical Society, 2018, 140, 6883-6892.	13.7	45
15	Sensing performance of thermoelectric hydrogen sensor for breath hydrogen analysisâ~†. Sensors and Actuators B: Chemical, 2009, 137, 524-528.	7.8	43
16	Effects of High-Humidity Aging on Platinum, Palladium, and Gold Loaded Tin Oxide—Volatile Organic Compound Sensors. Sensors, 2010, 10, 6513-6521.	3.8	42
17	Transmission electron microscope observation of the high-pressure form of magnesite retrieved from laser heated diamond anvil cell. Earth and Planetary Science Letters, 2005, 239, 98-105.	4.4	39
18	New Structural Design of Micro-Thermoelectric Sensor for Wide Range Hydrogen Detection. Journal of the Ceramic Society of Japan, 2006, 114, 853-856.	1.3	39

#	Article	IF	CITATIONS
19	Formation mechanism of monodispersed spherical core–shell ceria/polymer hybrid nanoparticles. Materials Research Bulletin, 2011, 46, 1168-1176.	5.2	39
20	Effects of noble metal addition on response of ceria thick film CO sensors. Sensors and Actuators B: Chemical, 2012, 171-172, 350-353.	7.8	33
21	Copper–manganese mixed oxides: CO ₂ -selectivity, stable, and cyclic performance for chemical looping combustion of methane. Physical Chemistry Chemical Physics, 2014, 16, 19634-19642.	2.8	31
22	Controlled Synthesis of Monodispersed Cerium Oxide Nanoparticle Sols Applicable to Preparing Ordered Self-Assemblies. Bulletin of the Chemical Society of Japan, 2008, 81, 761-766.	3.2	29
23	Phase boundary between rutile-type and CaCl ₂ -type germanium dioxide determined by in situ X-ray observations. American Mineralogist, 2002, 87, 99-102.	1.9	28
24	Selective Oxidation of Thioanisole with Hydrogen Peroxide using Copper Complexes Encapsulated in Zeolite: Formation of a Thermally Stable and Reactive Copper Hydroperoxo Species. ACS Catalysis, 2018, 8, 2645-2650.	11.2	28
25	VOCs sensing properties of layered organic–inorganic hybrid thin films: MoO3 with various interlayer organic components. Materials Letters, 2008, 62, 3021-3023.	2.6	26
26	Resistive Oxygen Sensor Using Ceria-Zirconia Sensor Material and Ceria-Yttria Temperature Compensating Material for Lean-Burn Engine. Sensors, 2009, 9, 8884-8895.	3.8	26
27	Long-term stability of Pt/alumina catalyst combustors for micro-gas sensor application. Journal of the European Ceramic Society, 2008, 28, 2183-2190.	5.7	25
28	Fabrication of thermoelectric gas sensors on micro-hotplates. Sensors and Actuators B: Chemical, 2009, 139, 340-345.	7.8	25
29	Thermopile sensor-devices for the catalytic detection of hydrogen gas. Sensors and Actuators B: Chemical, 2008, 130, 200-206.	7.8	23
30	Integration of ceramic catalyst on micro-thermoelectric gas sensor. Sensors and Actuators B: Chemical, 2006, 118, 283-291.	7.8	22
31	CO oxidation performance of Au/Co3O4 catalyst on the micro gas sensor device. Catalysis Today, 2013, 201, 85-91.	4.4	22
32	Improved catalytic activity of PrMO ₃ (M = Co and Fe) perovskites: synthesis of thermally stable nanoparticles by a novel hydrothermal method. New Journal of Chemistry, 2015, 39, 2342-2348.	2.8	22
33	Micro-thermoelectric devices with ceramic combustors. Sensors and Actuators A: Physical, 2006, 130-131, 411-418.	4.1	20
34	Thermoelectric gas sensor with CO combustion catalyst for ppm level carbon monoxide detection. Sensors and Actuators B: Chemical, 2013, 182, 789-794.	7.8	19
35	Selective hydroxylation of cyclohexene over Fe-bipyridine complexes encapsulated into Y-type zeolite under environment-friendly conditions. Catalysis Today, 2015, 242, 261-267.	4.4	19
36	Determination of Effective Oxygen Adsorption Species for CO Sensing Based on Electric Properties of Indium Oxide. Journal of the Electrochemical Society, 2018, 165, B275-B280.	2.9	19

#	Article	IF	CITATIONS
37	Thermoelectric hydrogen sensors using Si and SiGe thin films with a catalytic combustor. Journal of the Ceramic Society of Japan, 2010, 118, 188-192.	1.1	17
38	High-Temperature Thermoelectric Measurement of B-Doped SiGe and Si Thin Films. Materials Transactions, 2009, 50, 1596-1602.	1.2	16
39	Planar-type thermoelectric micro devices using ceramic catalytic combustor. Current Applied Physics, 2011, 11, S36-S40.	2.4	16
40	Development of highly sensitive mechanoluminescent sensor aiming at small strain measurement. Journal of Advanced Dielectrics, 2014, 04, 1450016.	2.4	16
41	Bisâ€Copper(II)/İ€â€Radical Multiâ€Heterospin System with Nonâ€innocent Doubly <i>N</i> â€Confused Dioxohexaphyrin(1.1.1.1.0) Ligand. Chemistry - A European Journal, 2017, 23, 15322-15326.	3.3	16
42	Solvent free oxidative coupling polymerization of 3-hexylthiophene (3HT) in the presence of FeCl ₃ particles. RSC Advances, 2016, 6, 111993-111996.	3.6	15
43	Monitoring Breath Hydrogen Using Thermoelectric Sensor. Sensor Letters, 2011, 9, 684-687.	0.4	15
44	Thermoelectric Gas Sensor using Au Loaded Titania CO Oxidation Catalyst. Journal of the Ceramic Society of Japan, 2007, 115, 37-41.	1.3	14
45	Fabrication and performance of free-standing hydrogen gas sensors. Sensors and Actuators B: Chemical, 2008, 129, 1-9.	7.8	14
46	Preparation of core-shell type cerium oxide/polymer hybrid nanoparticles for ink-jet printing. Journal of the Ceramic Society of Japan, 2009, 117, 769-772.	1.1	13
47	Physicochemical properties and microstructures of core-shell type cerium oxide/organic polymer nanospheres. Journal of the Ceramic Society of Japan, 2009, 117, 773-776.	1.1	13
48	Xâ€ray absorption fine structure study on the role of solvent on polymerization of 3â€hexylthiophene with solid FeCl ₃ particles. Journal of Polymer Science Part A, 2015, 53, 2075-2078.	2.3	11
49	Catalyst Combustors with B-Doped SiGe/Au Thermopile for Micro-Power-Generation. Japanese Journal of Applied Physics, 2006, 45, L1130-L1132.	1.5	10
50	13C CP/MAS NMR Study of Cross-linked Poly(vinylpyrrolidone) on Surface of Cerium Oxide Nanoparticles. Chemistry Letters, 2008, 37, 1116-1117.	1.3	10
51	Preparation of High-Density Polymer Brushes with a Multihelical Structure. Langmuir, 2018, 34, 3283-3288.	3.5	10
52	Analytical Study of Resistance Drift Phenomena on (PANI) <i>x</i> MoO3 Hybrid Thin Films as Gas Sensors. Bulletin of the Chemical Society of Japan, 2008, 81, 1331-1335.	3.2	9
53	Solvent-free, improved synthesis of pure bixbyite phase of iron and manganese mixed oxides as low-cost, potential oxygen carrier for chemical looping with oxygen uncoupling. Pure and Applied Chemistry, 2017, 89, 511-521.	1.9	9
54	Soot oxidation performance with a HZSM-5 supported Ag nanoparticles catalyst and the characterization of Ag species. RSC Advances, 2017, 7, 43789-43797.	3.6	9

#	Article	IF	CITATIONS
55	Depth-Resolved Characterization of Perylenediimide Side-Chain Polymer Thin Film Structure Using Grazing-Incidence Wide-Angle X-ray Diffraction with Tender X-rays. Langmuir, 2018, 34, 8516-8521.	3.5	9
56	Practical Test Methods for Hydrogen Gas Sensor Response Characterization. Electrochemistry, 2006, 74, 315-320.	1.4	8
57	Characterizations of interlayer organic–inorganic nanohybrid of molybdenum trioxide with polyaniline and poly(o-anisidine). Materials Chemistry and Physics, 2008, 110, 115-119.	4.0	8
58	XPS study of organic/MoO3 hybrid thin films for aldehyde gas sensors: correlation between average Mo valence and sensitivity. Journal of the Ceramic Society of Japan, 2010, 118, 171-174.	1.1	8
59	Formation of Tetravalent Fe Ions in LaFeO ₃ Perovskite Through Mechanochemical Modification by Ball Milling. Journal of the American Ceramic Society, 2015, 98, 1047-1051.	3.8	8
60	Monitoring of dispensed fluid with the quartz crystal microbalance (QCM) for the better control of inkjet or dispenser machine. Journal of the Ceramic Society of Japan, 2008, 116, 459-461.	1.1	7
61	Ceramic catalyst combustors of Pt-loaded-alumina on microdevices. Journal of the Ceramic Society of Japan, 2009, 117, 659-665.	1.1	7
62	Preparation and characterization of Pd loaded Sr-deficient K2NiF4-type (La, Sr)2MnO4 catalysts for NO–CO reaction. Catalysis Today, 2015, 251, 7-13.	4.4	7
63	Thermoelectric gas sensors with selective combustion catalysts. Journal of the Ceramic Society of Japan, 2019, 127, 57-66.	1.1	7
64	Morphology, microstructure, and surface area of La-added MgFe ₂ O ₄ powder. Journal of the Ceramic Society of Japan, 2018, 126, 402-407.	1.1	7
65	B- and P-Doped Si _{0.8} Ge _{0.2} Thin Film Deposited by Helicon Sputtering for the Micro-Thermoelectric Gas Sensor. Key Engineering Materials, 2006, 320, 99-102.	0.4	6
66	Highly Aldehyde Gas-Sensing Responsiveness and Selectivity of Layered Organic-Guest/MoO3-Host Hybrid Sensor. Journal of the Ceramic Society of Japan, 2007, 115, 742-744.	1.1	6
67	Microgenerator Using BiSbTe-Pt Thermopile and Pt-Al2O3 Ceramic Combustor. Journal of Electronic Materials, 2011, 40, 817-822.	2.2	6
68	Quantitative evaluation of the intratumoral distribution of platinum in oxaliplatinâ€ŧreated rectal cancer: <i>In situ</i> visualization of platinum <i>via</i> synchrotron radiation Xâ€ray fluorescence spectrometry. International Journal of Cancer, 2020, 146, 2498-2509.	5.1	6
69	Calibration Gas Preparation for Non-Disposable Portable MOx, PID, and IER VOC Detectors. Sensor Letters, 2012, 10, 985-992.	0.4	6
70	Preparation of Micro-Thermoelectric Hydrogen Sensor Loading Two Kinds of Catalysts to Enhance Gas Selectivity. Journal of the Ceramic Society of Japan, 2007, 115, 748-750.	1.1	5
71	Analysis of the dynamic behavior and local structure of solid-solution carbon in age-hardened low-carbon steels by soft X-ray absorption spectroscopy. Materialia, 2020, 14, 100876.	2.7	5
72	Alternating Current Impedance Analysis of CeO ₂ Thick Films as Odor Sensors. Sensor Letters, 2011, 9, 703-705.	0.4	5

#	Article	IF	CITATIONS
73	Thermoelectric hydrogen gas sensor. Synthesiology, 2011, 4, 99-107.	0.2	4
74	Control of crystal structure and performance evaluation of multi-piezo material of Li _{1â^²} <i>_x</i> Na <i>_x<!--<br-->Journal of the Ceramic Society of Japan, 2020, 128, 518-522.</i>	i&g tt,N bO8	klt;sub>3&
75	Uniform Organically Modified CeO ₂ Nanoparticles Synthesized from a Carboxylate Complex under Supercritical Hydrothermal Conditions: Impact of Ce Valence. Journal of Physical Chemistry C, 2022, 126, 6008-6015.	3.1	4
76	Temperature-programmed Desorption of Oxygen from La–Sr–Co–Fe Perovskite in Atmospheres with Varying Oxygen Partial Pressure. Chemistry Letters, 2015, 44, 357-359.	1.3	3
77	High Performance of SnO2-Based Gas Sensor by Introducing Perovskite-Type Oxides. ECS Transactions, 2016, 75, 31-37.	0.5	3
78	Observation of Chemical State for Interstitial Solid Solution of Carbon in Low-carbon Steel by Soft X-ray Absorption Spectroscopy. Tetsu-To-Hagane/Journal of the Iron and Steel Institute of Japan, 2018, 104, 628-633.	0.4	3
79	PM oxidation over Ag-loaded perovskite-type oxide catalyst prepared by thermal decomposition of heteronuclear cyano-complex precursor. Catalysis Today, 2019, 332, 83-88.	4.4	3
80	Electrode contact study for SiGe thin film operated at high temperature. Applied Surface Science, 2008, 254, 4999-5006.	6.1	2
81	Micronization of MgFe ₂ O ₄ particles doped with Si. Journal of the Ceramic Society of Japan, 2016, 124, 777-780.	1.1	2
82	The difference of PMMAâ€brushâ€modification on the oxygen permeable perovskiteâ€ŧype oxides by consisting elements. Journal of the American Ceramic Society, 2021, 104, 4932-4937.	3.8	2
83	Microheater Meander Configurations for Combustion Catalysts in Thermoelectric Gas Sensor. Sensor Letters, 2010, 8, 792-800.	0.4	2
84	Thermoelectric Micro-Multi-Gas Sensor for the Detection of Hydrogen, Carbon Monoxide and Methane. Sensor Letters, 2011, 9, 773-777.	0.4	2
85	Pt Loaded Alumina Ceramic Catalysts for Micro Thermoelectric Hydrogen Sensors. Journal of the Ceramic Society of Japan, 2006, 114, 686-691.	1.3	1
86	Resistive Type Sensor Using Ceria Thick Film with Nano Particles. Advanced Materials Research, 2008, 47-50, 1522-1525.	0.3	1
87	Pt catalytic effects on a resistive oxygen sensor using Ce0.9Zr0.1O2 thick film in rich conditions. Journal of the Ceramic Society of Japan, 2010, 118, 175-179.	1.1	1
88	Thermoelectric gas sensors of different catalyst oxides and heater metals. IOP Conference Series: Materials Science and Engineering, 2011, 18, 212010.	0.6	1
89	Oxygen sorption-desorption properties and order–disorder transitions on La–Sr–Co–Fe perovskite-type oxides. Journal of the Ceramic Society of Japan, 2019, 127, 378-382.	1.1	1
90	Observation of Chemical State for Interstitial Solid Solution of Carbon in Low-carbon Steel by Soft X-ray Absorption Spectroscopy. ISIJ International, 2020, 60, 114-119.	1.4	1

#	Article	IF	CITATIONS
91	Surface Organic Modification of In ₂ O ₃ Nanoparticle Assemblies and Their Flammable Gas Sensing Properties. Science of Advanced Materials, 2011, 3, 853-858.	0.7	1
92	Soot Oxidation Activity of Ag/HZSM-5 (Si/Al=40) Catalyst. Evergreen, 2017, 4, 7-11.	0.5	1
93	Micro-Thermoelectric Gas Sensor with P-doped SiGe Thin Film Deposited by Helicon Sputtering. ECS Transactions, 2006, 1, 23-27.	0.5	0
94	Effect of Thermal Conductivity of Catalytic Materials on Soot Sensing Performance Based on a Combustion-type Sensor. Chemistry Letters, 2017, 46, 1304-1307.	1.3	0
95	Development of Hydrogen Sensors and Their Application to Monitoring of Human Condition. Journal of Japan Institute of Electronics Packaging, 2008, 11, 508-512.	0.1	Ο